RSC Advances

# Electrochemical synthesis of luminescent ferrous fluorosilicate hexahydrate ($FeSiF_6 \cdot 6H_2O$) nano-powders



| | |
|---|---|
| Journal: | *RSC Advances* |
| Manuscript ID | RA-COM-11-2015-025183.R1 |
| Article Type: | Communication |
| Date Submitted by the Author: | 06-Jan-2016 |
| Complete List of Authors: | Pastushenko, Anton; Nanotechnology Institute of Lyon, University Lyon 1, UMR CNRS 5270, INSA Lyon; Apollon Solar SAS,<br>Lysenko, V.; Nanotechnology Institute of Lyon, University Lyon 1, UMR CNRS 5270, INSA Lyon |
| Subject area & keyword: | Electrochemistry < Physical |
| | |

Journal Name

COMMUNICATION

# Electrochemical synthesis of luminescent ferrous fluorosilicate hexahydrate ($FeSiF_6{\cdot}6H_2O$) nano-powders

Received 00th January 20xx,
Accepted 00th January 20xx

DOI: 10.1039/x0xx00000x

www.rsc.org/

A. Pastushenko [*, a, b] and V. Lysenko [b]

**Being mainly studied as a high-spin iron (II) based compound, ferrous fluorosilicate (FFS) hexahydrate has never been described in literature as photoluminescent material. Electrochemical synthesis of strongly luminescent FFS nano-powder from bulk metallurgical $FeSi_2/Si$ substrates is reported in this letter. Main electrochemical/chemical mechanisms involved in the FFS formation are identified. Strong photoluminescence in red-yellow spectral region of the synthesized nano-powders is supposed to occur via relatively deep $Si$-related electronic defect states within FFS band gap.**

The ferrous fluorosilicate (FFS) hexahydrate is one of the best understood high-spin ferrous compounds [1]. It is known to have at room temperature a rhombohedral crystal structure ($\alpha = 97.1°$) belonging to the space group $R\bar{3}m$ [2]. In particular, it can be represented as a slightly distorted $CsCl$ structure with octahedral complexes $SiF_6^{2-}$ at the corners and a $Fe$ atom at the center surrounded by water molecules forming a $Fe(H_2O)_6^{2+}$ complex coupled by hydrogen bonds with $SiF_6^{2-}$ [2]–[4]. However, no study concerning luminescent properties of FFS has been reported. According to our experience, white FFS crystals chemically synthesized in a standard way [5] by mixing $Fe(OH)_2$ with aqueous $H_2SiF_6$ acid as pointed out by the following reaction:

$$Fe(OH)_2 + H_2SiF_6(aq.) \rightarrow FeSiF_6 \cdot 6H_2O \qquad (1)$$

have been found to be non-luminescent at room temperature.
In this letter, electrochemical synthesis of strongly luminescent FFS nano-powder from bulk metallurgical substrates composed by crystalline phases of iron disilicide ($FeSi_2$) and silicon ($Si$) ǂ is reported.
Electrochemical etching of the $FeSi_2/Si$ substrates was performed for $180\ min$ at low temperature ($-20\ °C$) in a PTFE anodization cell filled with the mixture $1:1$ (in volume) of hydrofluoric acid ($HF$) and ethanol ($C_2H_5OH$) under constant current mode ($100\ mA/cm^2$). A copper plate served as rear contact for the $FeSi_2/Si$ substrates. A platinum wire was used as a cathode. To prevent any heating of the etching solution, one second stop-etching pulse was applied after each one second period of current on-pulse. At the end of anodization, sample was carefully washed with ethanol, dried, and then scraped from the substrate. The yield of the product was estimated to be from 3.5 to 5.0 %, depending on anodization conditions used.
Characteristic XRD diffraction patterns of the initial $FeSi_2/Si$ substrate as well as of $FeSiF_6 \cdot 6H_2O$ nano-powder produced during the anodization procedure described above is shown in Figure 1. Peaks corresponding to the crystalline phases of $Si$, $FeSi_2$ and $FeSiF_6 \cdot 6H_2O$ are indicated on the XRD diagram by numbers 1, 2 and 3, respectively. The inset illustrates red-luminescent (under UV lamp excitation) round anodized zone on the $FeSi_2/Si$ substrate where the FFS has been formed.

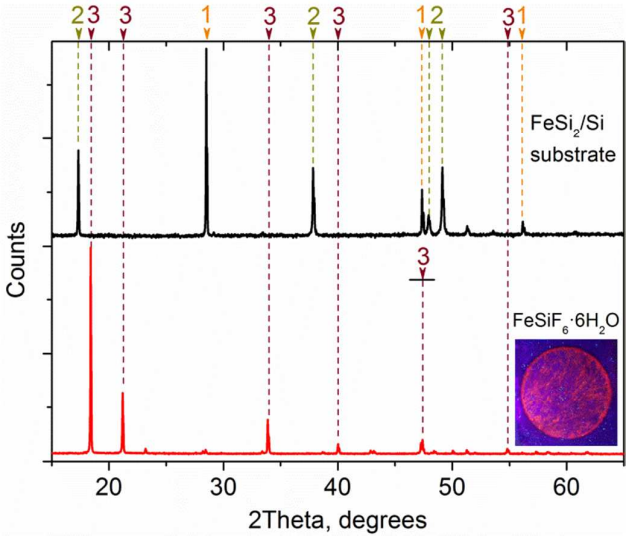


Figure 1. X-ray diffraction patterns of initial bulk metallurgical $FeSi_2/Si$ substrate (black curve) and electrochemically synthesized $FeSiF_6 \cdot 6H_2O$ powder (red curve). Peaks corresponding to the crystalline phases of $Si$, $FeSi_2$ and $FeSiF_6 \cdot 6H_2O$ are indicated on the XRD diagram by numbers 1, 2 and 3, respectively.

[a] Nanotechnology Institute of Lyon, University Lyon 1, UMR CNRS 5270, INSA Lyon, 7 avenue Jean Capelle, 69621 Villeurbanne, France
[b] Apollon Solar SAS, 66 Course Charlemagne, 69002 Lyon, France

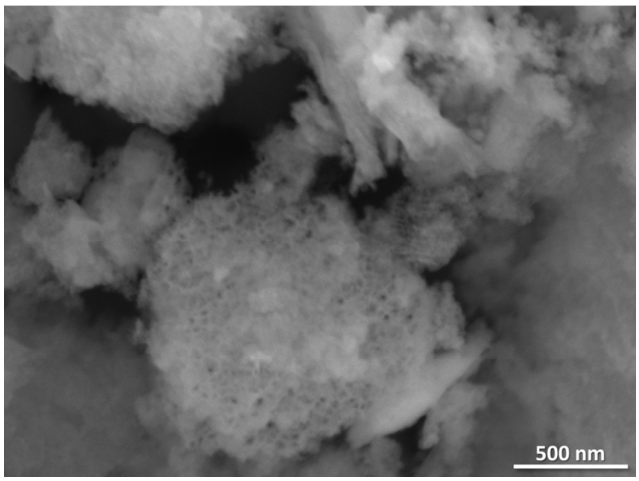


Figure 2. Scanning electronic microscopy image of the electrochemically synthesized $FeSiF_6 \cdot 6H_2O$ nano-powder.

Scanning electronic microscopy image of the obtained FFS nano-powder is shown in Figure 2 where numerous nanoscale flakes with porous morphology can be observed.

The white colour of the nano-flakes appeared due to the very easy electron-induced charging effect clearly reflects their dielectric nature.

Based on the first results reported above, the following electrochemical/chemical mechanisms can be involved in the FFS formation. First of all, one has to consider electrochemical etching of $Si$ in $HF$ solutions [6]–[8] summarized by the following equation:

$$Si + 2h^+ + 2F^- + 4HF \rightarrow H_2SiF_6 + H_2 \uparrow \qquad (2)$$

where $h^+$ depicts a valence band hole electrically injected in the anodized substrate and playing the role of an oxidizer of $Si$. As a result, hexafluorosilicic acid ($H_2SiF_6$) is formed and the electrochemical dissolution of $Si$ creates a nanoscale porous network facilitating chemical dissolution of iron disilicide according to the following reaction:

$$FeSi_2 + 2HF \rightarrow FeF_2 + H_2 \uparrow \qquad (3)$$

Chemical reaction between the formed iron fluoride ($FeF_2$) and hexafluorosilicic acid leads to formation of FFS nano-powder as described by reaction (4):

$$FeF_2 + H_2SiF_6 \rightarrow FeSiF_6 \cdot 6H_2O + 2HF \qquad (4)$$

In order to understand origins of the strong room temperature luminescence of the electrochemically synthesized FFS phase, steady-state and time-resolved photoluminescence (PL) spectral analysis has been performed. Figure 3-a shows a typical PL spectrum (black line) of the FFS powder obtained under low level excitation with a $Xe$ lamp (450 $W$ total output power in the 'white' range from 250 $nm$ to 1000 $nm$, 5 $nm$ excitation slit). Deconvolution of the spectrum with two Gaussian functions reveals: one dominant (1) and another low intensive (2) PL bands centred, respectively, at 2.06 $eV$ and 1.67 $eV$. The PL band 2 ensures an asymmetric shape of the overall PL spectrum. Typical PL transients are shown in Figure 3-b. Clear bi-exponential behaviour of the PL decays with rapid ($2-3$ µ$s$) and slow ($20-70$ µ$s$) components can be observed. The dominant PL band 1 is composed by rapid and slow electronic transitions with the characteristic lifetime values $\tau_1^r = 2-3$ µ$s$ and $\tau_1^s = 26$ µ$s$, respectively. As for the PL band 2, it is mainly characterized by a slow component with $\tau_2 = 70$ µ$s$ and only a weak rapid initial part of the corresponding PL transient can be seen. In summary, the higher the emission energy is, the more pronounced the rapid part is and time constant of the slow part significantly decreases. The rapid electronic transitions with the characteristic lifetime values $\tau_1^r = 2-3$ µ$s$ can be associated, for example, to non-radiative Auger recombination mechanism, which is much less pronounced at lower emission energies. Moreover, a high level photo-excitation of the FFS powder performed, for example, with a fs-laser (343 $nm$, pulse width $< 250$ $fs$, pulse energy: 20 $nJ$, repetition rate: 54 $MHz$) leads to domination of the low energy PL band 2 (see red PL spectrum in Figure 3-a).

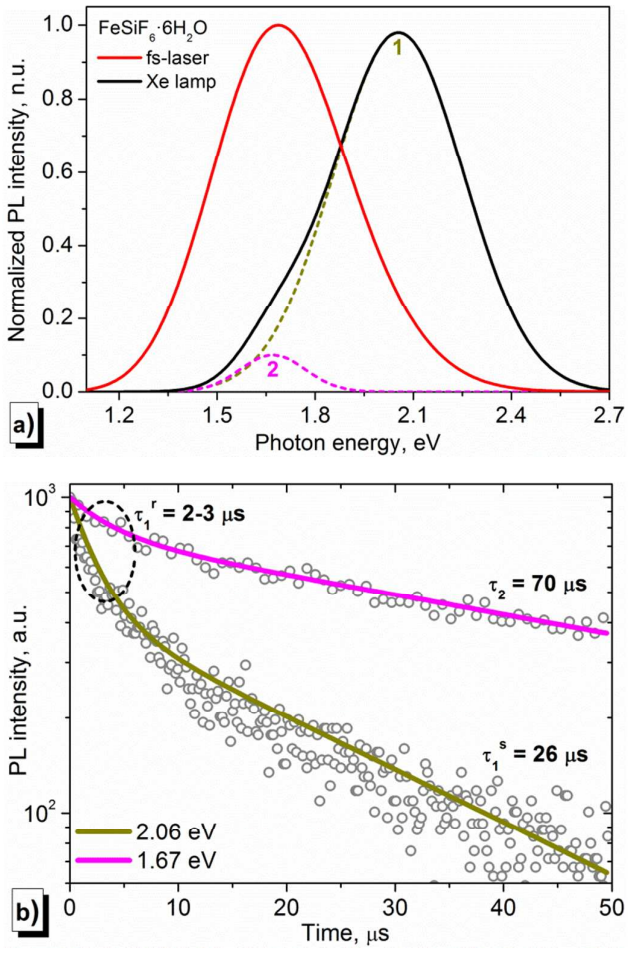


Figure 3. a) PL spectra of the FFS powder excited with a $Xe$ lamp (black line) and fs-laser (red line). b) Typical PL transients measured at 1.67 $eV$ and 2.06 $eV$ under excitation by a pulse laser (377 $nm$, pulse width 76 $ps$, pulse period 50 $\mu s$).

As we have already mentioned at the beginning of our communication, the FFS powder resulted from the purely chemical reaction (1) was found to be non-luminescent at room temperature.

However, when it is performed on a crystalline $Si$ wafer under a moderate heating up to $130\ °C$, bright spotty red PL of the $FeSiF_6 \cdot 6H_2O/Si$ interface under UV light excitation can be observed. Furthermore, the corresponding PL spectrum almost perfectly coincides with the PL spectrum of the electrochemically synthesized FFS nano-powder under the same photo-excitation ensured by the fs-laser (see Figure 4). It means that presence of the Si phase in the both chemical and electrochemical synthesis ways is of the first importance to ensure the high PL intensity of the FFS powder. In addition, centrifugation-induced size selection of the FFS nano-flakes dispersed in ethanol does not shift spectral maximum position of their PL signals (only integral PL intensity of the spectra progressively decreases). It means that the PL origin cannot be related to any size effect due to quantum confinement of photo generated charge carriers, for example, as it occurs for the cases of luminescent $Si$ or $SiC$ nanoparticles [9]–[11].

Taking into account that: (i) $Si$ play an important role in the high PL intensity of the FFS-based powders and (ii) there is no size dependence of their PL properties, we can suppose that the observed strong PL of the synthesized powders occurs via relatively deep electronic states formed by charged and neutral $Si$ containing species within the band gap of the slightly non-stoichiometric crystalline FFS phase (similar to the luminescent energy states created by $Si$ atoms in luminescent $SiN_x$ films [12], [13]). Actually, such species (for example: $SiF_6^-$, $SiF_6^0$) can appear from interaction of $SiF_6^{2-}$ ions situated in the corners of octahedral unit cell of FFS with the electrochemically formed external $Si^+$ ions.

In conclusions, luminescent $FeSiF_6 \cdot 6H_2O$-based nano-powders can be synthesized by anodization of low-cost metallurgical $FeSi_2/Si$ substrates in $HF/EtOH$ solutions.

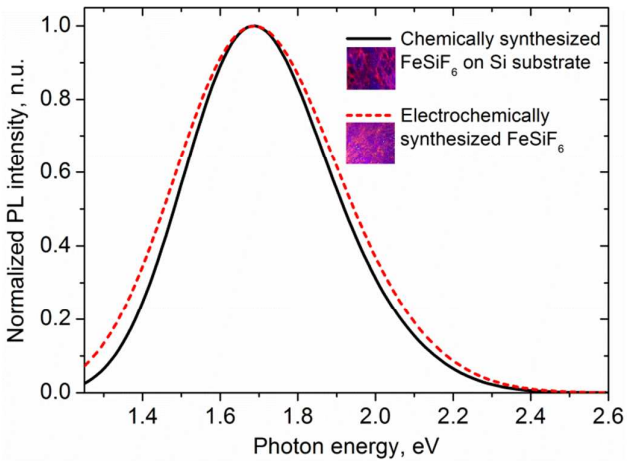


Figure 4. Room temperature PL spectra (under $343\ nm$ fs-laser excitation) of the FFS powder: (i) chemically synthesized on a bulk $Si$ substrate (black line) and (ii) electrochemically synthesized from the $FeSi_2/Si$ metallurgical substrates.

Despite of high concentration of various numerous impurities present in the original substrates, the final powder is found to be strongly luminescent contrary to the case of porous $Si$ nanostructures electrochemically grown on metallurgical $Si$ substrates. $Si$ phase has been found to play the main role in the luminescent properties of the $FeSiF_6 \cdot 6H_2O$ nano-powders because they are responsible for formation of the electronic states within the band gap of the obtained powders which are involved in radiative recombination of photo-generated charge carriers. Finally, the obtained material is chemically and photo stable: its storage at room temperature in ambient air for two years resulted in no visible changes to photoluminescence spectrum position and intensity.

## Acknowledgement

Apollon Solar company is acknowledged for financial support as well as for providing with the bulk metallurgical substrates in frames of this research work. The authors acknowledge Dr. Jed Kraiem, Dr. Oleksiy Nichiporuk and Dr. Tetyana Nychyporuk for fruitful discussion.

## Notes and references

‡ The original bulk $FeSi_2/Si$ substrates were provided by Apollon Solar company (France). The main impurities in the substrates concern: $Al$ (0.2%), $Ca$ (0.2%), $Ti$ (0.1%), $Mn$ (0.5%).

1 J. Krzystek, D. Smirnov, C. Schlegel, J. van Slageren, J. Telser, and A. Ozarowski, *J. Magn. Reson.*, 2011, 213, 158.
2 W. C. Hamilton, *Acta Crystallogr.*, 1962, **15**, 353.
3 G. Chevrier, A. Hardy, G. Jéhanno, *Acta Crystallogr. Sect. A*, 1981, **37**, 578.
4 G. Chevrier, *J. Solid State Chem.*, 1994, **111**, 322.
5 M. Grobelny, *J. Fluor. Chem.*, 1977, **9**, 409.
6 V. Lehmann, U. Gosele, *Appl. Phys. Lett.*, 1991, **58**, 856.
7 M. J. Sailor, *Porous Silicon in Practice*, Wiley-VCH Verlag & Co. KGaA, ISBN 978-3-527-64192-5, 2012.
8 L. Canham, *Handbook of Porous Silicon*, Springer International Publishing, ISBN 978-3-319-05743-9, 2014.
9 V. Lysenko, V. Onyskevych, O. Marty, V. A. Skryshevsky, Y. Chevolot, C. Bru-Chevallier, *Appl. Phys. Lett.*, 2008, **92**, 29.
10 J. Botsoa, J. M. Bluet, V. Lysenko, L. Sfaxi, Y. Zakharko, O. Marty, G. Guillot, *Phys. Rev. B*, 2009, **80**, 1.
11 T. Serdiuk, V. Lysenko, S. Alekseev, V. A. Skryshevsky, *J. Colloid Interface Sci.*, 2011, **364**, 65.
12 J. Robertson, M. J. Powell, *Appl. Phys. Lett.*, 1984, **44**, 415.
13 Y. Liu, Y. Zhou, W. Shi, L. Zhao, B. Sun, T. Ye, *Mater. Lett.*, 2004, **58**, 2397.

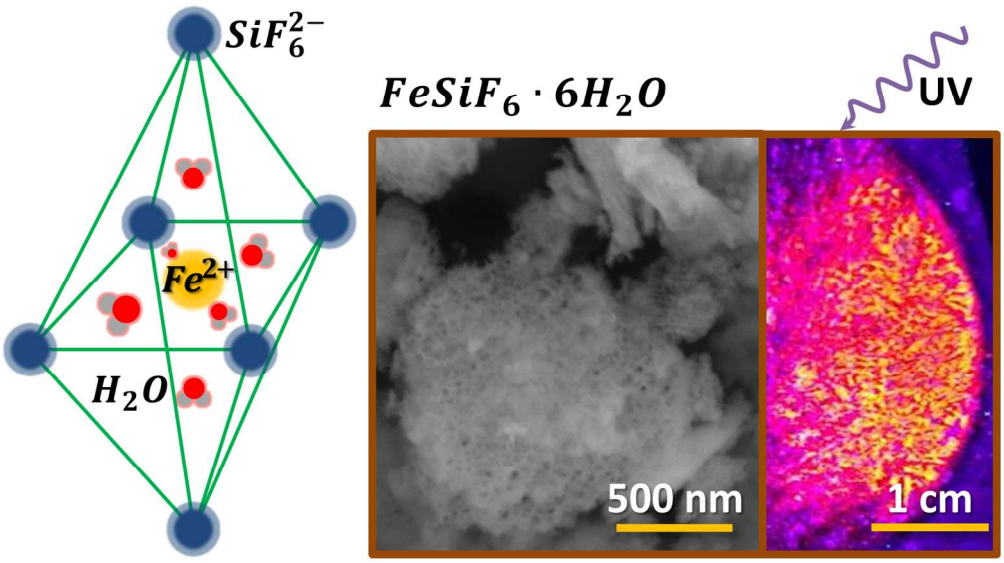


143x79mm (300 x 300 DPI)